



Gibson, G.M., Leach, J., Keen, S., Wright, A.J., and Padgett, M.J. (2008) *Measuring the accuracy of particle position and force in optical tweezers using high-speed video microscopy*. Optics Express, 16 (19). pp. 14561-14570. ISSN 1094-4087 (doi:10.1364/OE.16.014561)

<http://eprints.gla.ac.uk/32452/>

Deposited on: 11th September 2012

Measuring the accuracy of particle position and force in optical tweezers using high-speed video microscopy

Graham M Gibson^{1*}, Jonathan Leach¹, Stephen Keen¹,
Amanda J Wright² and Miles J Padgett¹

¹*Department of Physics and Astronomy, University of Glasgow, Glasgow G12 8QQ, UK.*

²*Institute of Photonics, SUPA, University of Strathclyde, Glasgow G4 0NW, UK.*

[*g.gibson@physics.gla.ac.uk](mailto:g.gibson@physics.gla.ac.uk)

Abstract: We assess the performance of a CMOS camera for the measurement of particle position within optical tweezers and the associated autocorrelation function and power spectrum. Measurement of the displacement of the particle from the trap center can also be related to the applied force. By considering the Allan variance of these measurements, we show that such cameras are capable of reaching the thermal limits of nanometer and femtonewton accuracies, and hence are suitable for many of the applications that traditionally use quadrant photodiodes. As an example of a multi-particle measurement we show the hydrodynamic coupling between two particles.

© 2008 Optical Society of America

OCIS codes: (140.7010) Laser trapping; (170.4520) Optical confinement and manipulation; (350.4855) Optical tweezers or optical manipulation.

References and links

1. A. Ashkin, J. M. Dziedzic, J. E. Bjorkholm, and S. Chu, "Observation of a single-beam gradient force optical trap for dielectric particles," *Opt. Lett.* **11**, 288–290 (1986).
2. J. E. Molloy and M. J. Padgett, "Lights, action: optical tweezers," *Contemp. Phys.* **43**, 241–258 (2002).
3. J.-C. Meiners and S. R. Quake, "Femtonewton force spectroscopy of single extended DNA molecules," *Phys. Rev. Lett.* **84**, 5014–5017 (2000).
4. K. C. Neuman and S. M. Block, "Optical trapping," *Rev. Sci. Instrum.* **75**, 2787–2809 (2004).
5. M. Polin, D. G. Grier, and S. R. Quake, "Anomalous vibrational dispersion in holographically trapped colloidal arrays," *Phys. Rev. Lett.* **96**, 088101 (2006).
6. S. Keen, J. Leach, G. Gibson, and M. Padgett, "Comparison of a high-speed camera and a quadrant detector for measuring displacements in optical tweezers," *J. Opt. A: Pure Appl. Opt.* **9**, S264–S266 (2007).
7. O. Otto, C. Gutsche, F. Kremer, and U. F. Keyser, "Optical tweezers with 2.5kHz bandwidth video detection for single-colloid electrophoresis," *Rev. Sci. Instrum.* **79**, 023710 (2008).
8. D. W. Allan, "Statistics of atomic frequency standards," *Proc. IEEE* **54**, 221–230 (1966).
9. J. Leach, K. Wulff, G. Sinclair, P. Jordan, J. Courtial, L. Thomson, G. Gibson, K. Karunwi, J. Cooper, Z. J. Laczik, and M. Padgett, "Interactive approach to optical tweezers control," *Appl. Opt.* **45**, 897–903 (2006).
10. G. Gibson, D. M. Carberry, G. Whyte, J. Leach, J. Courtial, J. C. Jackson, D. Robert, M. Miles, and M. Padgett, "Holographic assembly workstation for optical manipulation," *J. Opt. A: Pure Appl. Opt.* **10**, 044009 (2008).
11. K. Berg-Sørensen and H. Flyvbjerg, "Power spectrum analysis for optical tweezers," *Rev. Sci. Instrum.* **75**, 594–612 (2004).
12. J. R. Moffitt, Y. R. Chemla, D. Izhaky, and C. Bustamante, "Differential detection of dual traps improves the spatial resolution of optical tweezers," *PNAS* **103**, 9006–9011 (2006).
13. M. Klein, M. Andersson, O. Axner, and E. Fällman, "Dual-trap technique for reduction of low-frequency noise in force measuring optical tweezers," *Appl. Opt.* **46**, 405–412 (2007).

14. M. Atakhorrami, K. M. Addas, and C. F. Schmidt, "Twin optical traps for two-particle cross-correlation measurements: Eliminating cross-talk," *Rev. Sci. Instrum.* **79**, 043103 (2008).
 15. J.-C. Meiners and S. R. Quake, "Direct measurement of hydrodynamic cross correlations between two particles in an external potential," *Phys. Rev. Lett.* **82**, 2211–2214 (1999).
 16. C. D. Saunter, G. D. Love, M. Johns, and J. Holmes, "FGPA technology for high-speed, low-cost adaptive optics," vol. 6018 of *5th International Workshop on Adaptive Optics for Industry and Medicine* (SPIE, 2005).
 17. R. Di Leonardo, S. Keen, J. Leach, C. D. Saunter, G. D. Love, G. Ruocco, and M. J. Padgett, "Eigenmodes of a hydrodynamically coupled micron-size multiple-particle ring," *Phys. Rev. E* **76**, 061402 (2007).
-

1. Introduction

For 20 years, optical tweezers[1] have found numerous applications in biology ranging from the manipulation of live bacteria and viruses to measuring the forces between micrometer sized particles or even cells[2]. Forces acting on the trapped particle are measured in one of two ways. Firstly, the trap position is fixed and the observed displacement of the particle is related to a force by the stiffness of the trap. Secondly, the trap position is constantly updated such that the particle does not move, and the force is deduced from the required displacement of the trap. Both techniques require a precise, accurate and high-bandwidth measurement of the trapped particle position. In this work we concentrate on the first technique - simply demonstrating the potential of high-speed CMOS cameras.

In many biological applications, transparent beads are attached to a particle under study, thus acting as "handles", that can be used to manipulate the particle. Precise determination of the position of the trapped particle, typically to nanometer resolution, is required to measure the forces in many biological systems at the sub-piconewton scale[3].

The position of trapped particles has traditionally been measured using either a quadrant photodiode (QPD)[4] or standard video camera with particle tracking software[5]. QPDs are the common choice for measuring force since they offer precise, high-bandwidth measurements, typically several kHz, whereas standard video cameras are limited by acquisition rates of only 10's of Hz. Standard video frame rates are thus too slow compared to the characteristic frequency of the optical trap. However, video cameras are convenient and allow multiple particles to be tracked simultaneously, over large fields of view. High-speed cameras offer an alternative solution, allowing measurement rates of several kHz. Reference[6] shows similar performance for both a high-speed, full-field, CCD camera and a QPD for displacement measurements in optical tweezers. However, since the total data of the image sequence is large, measurement time is usually limited to a few seconds due to the available on-board memory storage, after which the data needs to be downloaded to the computer. A solution that looks more promising involves the use of CMOS cameras, that can provide reduced field of view (horizontal and vertical) frame rates of the order 1kHz, and the data can be managed in real time using a standard desktop PC[7].

In this paper we investigate the precision of position and force measurements in optical tweezers using a CMOS camera. We use the Allan variance [8] to characterize the stabilities of the measurements and determine the optimal trapping power and measurement, or calibration, time for a particular application. In addition we compare single and dual trapping techniques.

2. Experimental configuration

Figure 1 shows a schematic representation of the experiment. Trapping is achieved using a CW Ti:sapphire laser system (M², SolsTiS) which provides up to 1W at 830nm. The laser is expanded to slightly overfill the aperture of a spatial light modulator (SLM) (Hamamatsu, LCOS X10468-02), allowing multiple optical traps to be created, and then coupled into the tweezers system by imaging the SLM on to the back aperture of the microscope objective lens. The device is gamma corrected such that approximately 60% of the incident light is diffracted

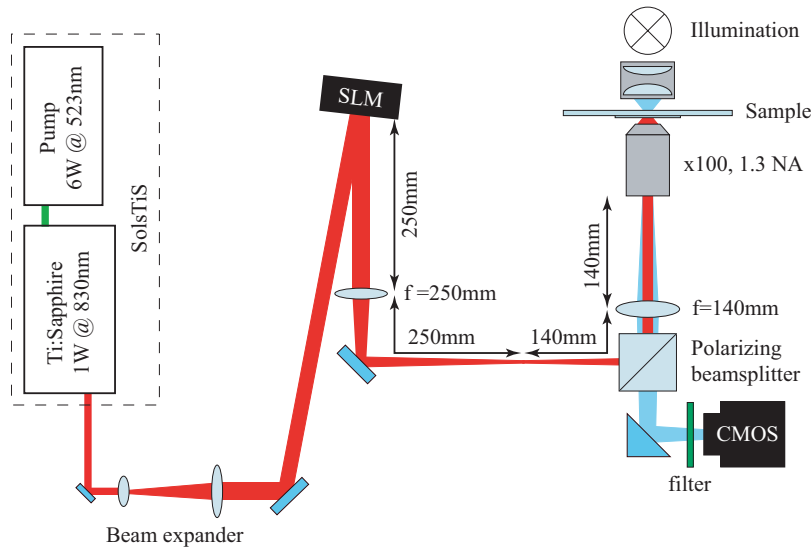


Fig. 1. The tweezers system is based around an inverted microscope. A titanium sapphire laser provides up to 1W @ 830nm, which is expanded to fill the aperture of an SLM. SLM control software allows the creation of multiple optical traps, coupled into the tweezers using a polarizing beamsplitter. The motion of trapped particles in the sample is analyzed using a CMOS camera.

into the desired trap pattern. Using our SLM control software [9, 10] we can trap one, or many, $2\mu\text{m}$ diameter silica beads and position them anywhere within the field of view. The tweezers is based around an inverted microscope, where the same objective lens, 100x 1.3NA, (Zeiss, Plan-Neofluor) is used to both focus the trapping beam and to image the resulting motion of the particles. Samples containing $2\mu\text{m}$ diameter silica beads in water are mounted in a motorized microscope stage (ASI, MS-2000). The stage allows accurate control of the sample position and provides a known displacement of a fixed particle, or bead, for calibrating the camera.

A 50W tungsten-halogen lamp and condenser is used to illuminate the sample, imaged using a CMOS camera (Prosilica, EC 1280). The camera is connected to a desktop PC using a firewire interface such that the images can be acquired and the particle motion analyzed. The magnification of the system corresponds to a scale of 13 pixels per micron. A polarizing beamsplitter reflects the trapping laser beam into the microscope objective while transmitting the white light image, allowing it to be viewed using the camera. A narrow-band filter prevents the camera being saturated by the trapping laser. The individual images are processed using our own LabVIEW (National Instruments) particle tracking software. Selecting a region of interest (ROI), such that the field of view of the camera is restricted to only image the particles under study, increases the frame rate. In the work presented here the ROI was reduced to approximately 40 square microns, allowing images to be taken at 1kHz with a corresponding shutter speed of 1ms. Shorter shutter speeds are possible, but serve no purpose since the decrease in image brightness results in a degraded accuracy of particle position measurement. The software allows further regions of interest to be defined e.g. regions around each particle in a multiple trap configuration. Each sub-ROI has an associated threshold value that can be set to reject the background field and the resulting images are processed using a center of mass algorithm to determine the particle position. Even with a standard desktop PC it is possible to obtain and record the particle position in real time, i.e. 1kHz. Calibration of the system was achieved us-

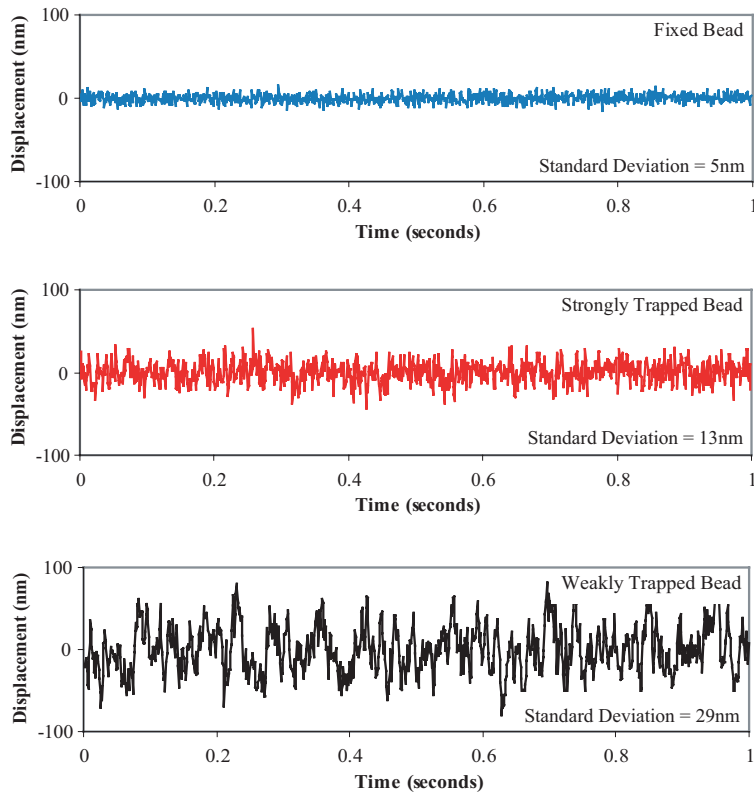


Fig. 2. Lateral displacement for a $2\mu\text{m}$ silica bead fixed to the coverslip and $2\mu\text{m}$ silica beads trapped with low and high laser power. Weak trap (7mW, $\kappa = 5.6\text{E-}6$ N/m), strong trap (37mW, $\kappa = 2.3\text{E-}5$ N/m).

ing the motorized microscope stage to move a fixed bead over a known distance, allowing the camera to be calibrated in pixels / μm .

The complete optical system is mounted on an air damped optical table in order to isolate the system from environmental sources of noise. In addition, the optical components are mounted as close to the table as practically possible in order to reduce effects from mechanical resonance.

3. Position measurements, autocorrelations and power spectra

Fluctuations in the measurement of particle position within optical tweezers arise from two possible sources. Firstly there is noise from the sensor, and secondly that the particle itself is subject to random thermal motion. Since both these sources of variation are approximated by a Gaussian distribution of measurement position, some care is required to distinguish between them.

In principle, the motion of a trapped particle is simply that of a thermally excited, over-damped oscillator in a harmonic potential characterized by a spring stiffness κ [2, 11]. The size of the residual Brownian motion $\langle x^2 \rangle$ is given by the equipartition of energy [11],

$$\frac{1}{2}k_B T = \frac{1}{2}\kappa \langle x^2 \rangle. \quad (1)$$

Indeed, measuring $\langle x^2 \rangle$ is a common method for deducing κ . Since the oscillator is significantly

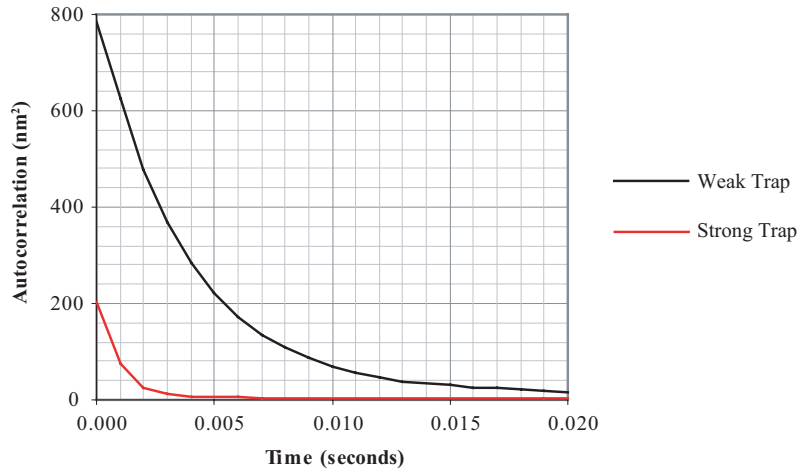


Fig. 3. Autocorrelation of position for a $2\mu\text{m}$ silica bead trapped with low and high laser power.

over damped, the autocorrelation of particle position is described by a single exponential decay of time constant $\tau_0 = 1/2\pi f_0$, where f_0 is the knee frequency above which the particle can be considered to be free, given by [11]

$$f_0 = \frac{\kappa}{2\pi\gamma} \quad (2)$$

where $\gamma = 6\pi r\eta$, η is the viscosity of the surrounding fluid and r is the radius of the particle.

Figure 2 shows the lateral displacement as measured from the camera image as a function of time for a bead fixed to the coverslip and beads trapped with low and high laser power. The apparent standard deviation of the fixed particle is of order 5nm, significantly smaller than that of the trapped beads which have standard deviations of 29nm and 13nm for the low ($\kappa = 5.6\text{E-}6$ N/m) and high ($\kappa = 2.3\text{E-}5$ N/m) trap strengths respectively. This shows that the camera system is sufficient for measuring the thermal motion of the trapped particles, easily distinguished from the sensor noise revealed by the fixed particle. Alternatively, the thermal motion of the trapped particles is often studied by plotting the autocorrelation (Fig. 3) or power spectrum (Fig. 4). However, although sufficient for some applications, none of these results show how the sensor performance varies over differing averaging timescales, nor over which timescales the sensor reaches a performance level sufficient to record the true thermal motion of the particles.

4. Allan variance of position measurements

When accessing the performance of a generic measurement system, it is convenient to consider the Allan variance of the, nominally constant, sensor output. The Allan variance indicates the timescales over which the system is dominated by Gaussian noise or drift. At short timescales the variation in output is dominated by the noise in the sensor, or the true fluctuations in the system. Both of these fluctuations are Gaussian distributed and hence averaging the data over longer time-windows gives an improvement in the reproducibility of the average value, which improves in proportion to the square root of the number of measurements. At longer timescales, the measurement system is usually subject to drift and averaging the output over these longer time windows ceases to yield any improvement in the reproducibility of the mean value. This transition between the two regimes indicates the useful time over which the system can be said

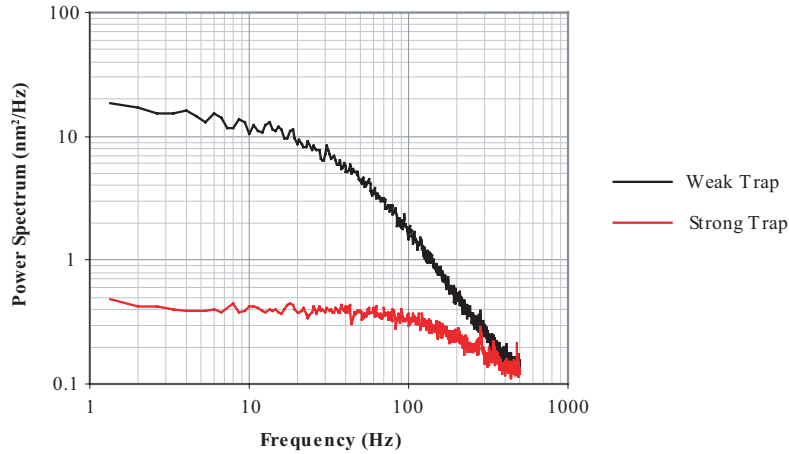


Fig. 4. Power Spectra of position for a $2\mu\text{m}$ silica bead trapped with low and high laser power.

to be stable.

Using the particle tracking method described above we recorded the xy positions of trapped silica beads over a duration of 5 minutes (300,000 data points). From the xy data we calculated the Allan variance of position given by

$$\sigma_x^2(\tau) = \frac{1}{2} \langle (x_{n+1} - x_n)^2 \rangle \quad (3)$$

where x_n is the average position over the sample period n , and τ is the time per sample period.

When averaged over multiple measurements, the standard error of the average position of the trapped particle is dependent upon $\langle x^2 \rangle$ and the number of independent measurements, N . In a time Δt , the number of independent measurements is given by

$$N \approx \frac{\Delta t}{\sqrt{2}\tau_0} = \frac{\kappa\Delta t}{\sqrt{2}\gamma} \quad (4)$$

giving the standard error of the particle position, $SE_{\langle x \rangle}$, to be

$$SE_{\langle x \rangle} = \sqrt{\frac{\langle x^2 \rangle}{N}} \approx \sqrt{\frac{\sqrt{2}k_B T \gamma}{\kappa^2 \Delta t}}. \quad (5)$$

This limit cannot be bettered by any measurement system, it is a limit inherent in the random nature of Brownian motion. Averaging for longer times should, in principle, give ever better estimates of average particle position. However, it is difficult to completely isolate the trap from environmental sources of noise such as laser pointing stability and thermal drift of the microscope alignment. Various methods have been implemented to reduce such noise and include the development of dual trap techniques[12, 13, 14] where a second trapped particle is measured simultaneously. Since the drift affects both particles it can be eliminated from the data.

The plots in Fig. 5 show the Allan variance of the measured position, $\sigma_x^2(\tau)$, of a $2\mu\text{m}$ silica bead for different values of optical trap stiffness. Also shown is the Allan variance for the differential position between two beads trapped $10\mu\text{m}$ apart. For comparison the stronger trapped

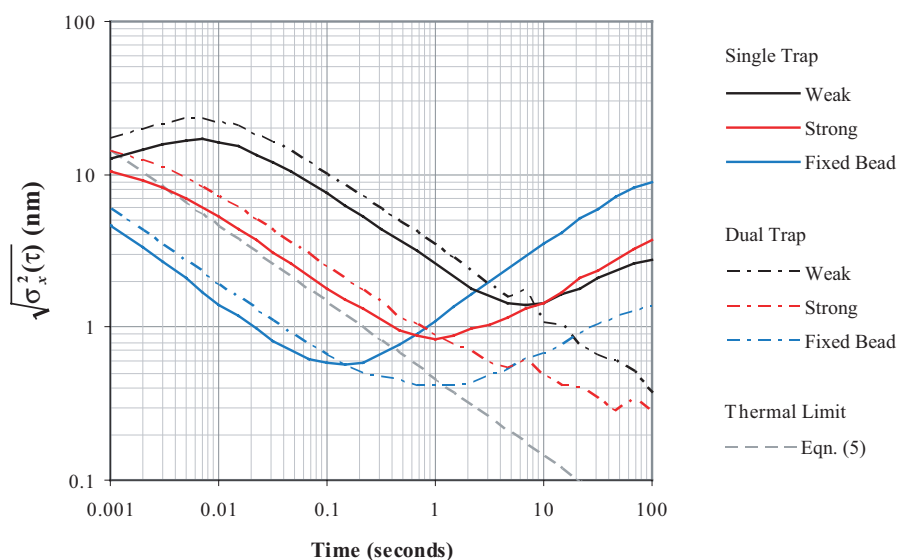


Fig. 5. Stability of position measurements. Increasing the trap power results in a higher measurement precision. For the case of a single bead measurement, the optimum averaging time is in the range 1-10 seconds. The blue lines correspond to the single and differential measurements of two $2\mu\text{m}$ silica beads that were fixed to the microscope coverglass, having a separation comparable to the trapped beads. The thermal limit is estimated for the strongly trapped bead. Weak trap (7mW, $\kappa = 5.6\text{E-}6$ N/m), strong trap (37mW, $\kappa = 2.3\text{E-}5$ N/m).

bead is plotted in relation to the estimate for the thermally limited precision given by Eq. 5. At timescales short compared to the autocorrelation time of the trap, the bead is moving with a uniform velocity and hence the Allan variance increases with time. At timescales above the autocorrelation time, the bead positions are randomly distributed within the trap and the accuracy of the mean improves with the square root of the averaging time. We see that for a single trap the minimum error is of order of 1nm obtained for an averaging time of order 1s. Above this time we see that the Allan variance increases, which is a result of drift within the system. The longer term stability of the system can be improved by making measurements on the differential position of two beads, which effectively drift together. However, this improvement in long term stability is only at the expense of a $\sqrt{2}$ increase in noise since the Brownian motion of the two beads add in quadrature. Shown also on the graph is the Allan variance of the position measurement of beads fixed to the cover slip. At short timescales the Allan variance is limited only by the inherent measurement noise of the camera technique, but at longer timescales it increases above that of the trapped bead. This increase at long timescales indicates that the thermal, or other, stability of the sample stage is worse than the pointing stability of the laser.

One possible concern on using a pixellated imaging sensor for precise position measurement is that the underlying pixellation may result in a systematic noise source that may mask sub-pixel information. In our system each pixel in the imaging sensor corresponds to approximately 77nm. One challenging application for position measurements within optical tweezers is the study of hydrodynamic coupling, which leads to subtle features in the position cross-correlation between trapped particles, corresponding to nanometer displacements [15]. The Allan variance results from Fig. 5 indicate that, for data collection times below a few seconds, the drift of

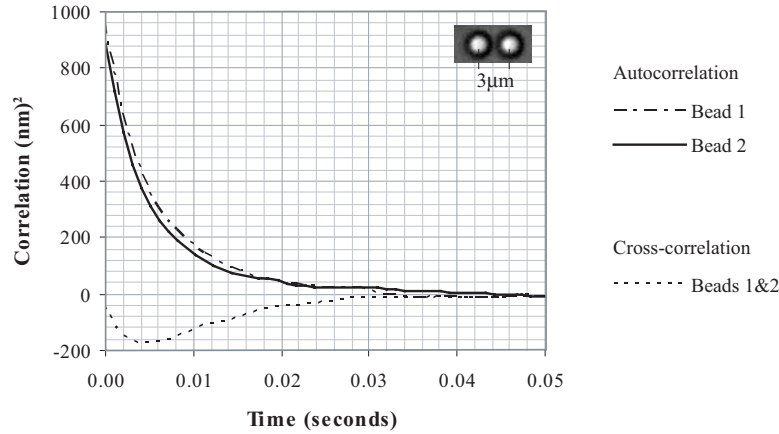


Fig. 6. Correlation graphs for two $2\mu\text{m}$ silica beads separated by $3\mu\text{m}$. The traces were averaged over 30 sequential data sets, each consisting of 2 seconds continuous data.

the system can be ignored. We therefore calculate the autocorrelation and cross-correlation of trapped particles from 2 seconds of continuous data, which we average over many sequential data sets to improve the overall signal to noise. Figure 6 shows autocorrelation and cross-correlation functions for two $2\mu\text{m}$ beads trapped $3\mu\text{m}$ apart, the traces are averaged over 30, 2 second data sets. We see that the functions are smoothly varying, showing no evidence of underlying “digitization” even at length scales $< 20\text{nm}^2$.

5. Allan variance of force measurements

Given that the position of the trapped particle can be precisely measured then an applied average force, $\langle F \rangle$, can be inferred from observation of the particle displacement from trap center, $\langle F \rangle = \kappa(\langle x \rangle - x_0)$, where both κ and x_0 can be determined from the positional data prior to the application of the force. Using the same data as for the standard error in the particle position, the equivalent standard error in the applied force is given as

$$SE_{\langle F \rangle} = SE_{\langle x \rangle} \kappa \approx \sqrt{\frac{\sqrt{2}k_B T \gamma}{\Delta t}}. \quad (6)$$

Note that although increasing κ increases the precision to which the particle position can be determined, it reduces the displacement for a given force. The result is a precision of thermally limited force measurement that is independent of κ .

The Allan variance of the measurements of force is given by $\sigma_F^2(\tau) = \sigma_x^2(\tau)\kappa^2$. The plots in Fig. 7 show the Allan variance of measurements of force acting on a $2\mu\text{m}$ silica bead for different values of κ . Also shown is the Allan variance for the differential force between two beads. For comparison these are plotted in relation to the estimate for the thermally limited precision given by Eq. 6. As discussed above, we see that for timescales longer than the autocorrelation time of the trap the precision of force measurement is independent of κ . At longer timescales the precision is compromised by the drift in the system. One sees that a force measurement precision of 10fN can be obtained for an averaging time of a few seconds.

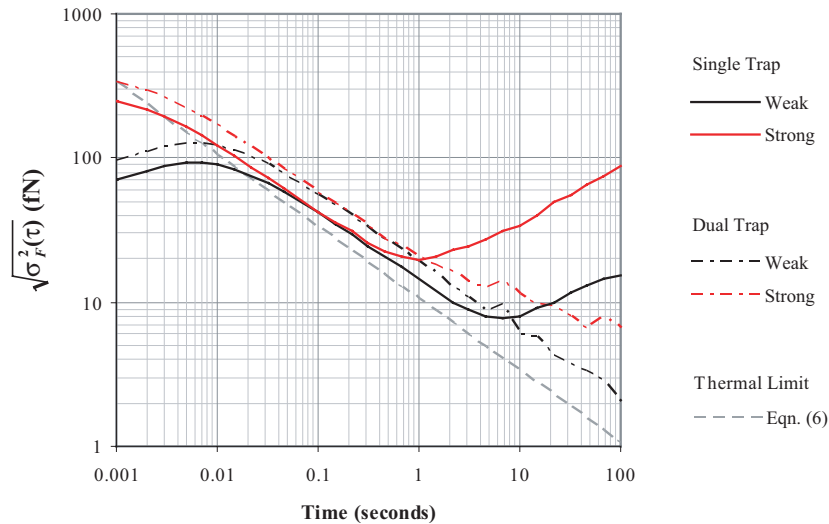


Fig. 7. Stability of force measurements. In contrast to the measurement of position, it is the weaker trap that results in a more precise measurement of force. As in the case of position measurement, the optimum measurement time is in the range 1-10 seconds. Weak trap (7mW, $\kappa = 5.6\text{E-}6$ N/m), strong trap (37mW, $\kappa = 2.3\text{E-}5$ N/m).

6. Discussion and conclusions

Irrespective of the precise sensor technology the Allan variance of the measurements is a useful indicator as to the stability and noise performance of the system. For our apparatus, built from conventional components and housed within a standard air-conditioned laboratory, it seems that a time scale of a few seconds represents the optimum compromise between averaging the Brownian motion whilst remaining insensitive to system drift. If greater precision is required then employing a differential system allows averaging over longer timescales, albeit a corresponding reduction in measurement bandwidth.

We have shown that CMOS imaging technology is capable of measuring the particle position and inferring the applied force with a precision limited only by the inherent thermal motion of the particle within an overdamped trap. Frame rates of 1kHz means that the overdamped motion is sampled sufficiently quickly that autocorrelation and cross-correlation measurements between multiple particles can be measured. Averaging position or force data over a few seconds gives standard errors in the mean of order 1nm and 10fN respectively. These values are also comparable with those reported for systems based on QPDs.

The nature of CMOS devices is that the maximum data transfer rate sets a limit on the product of frame-rate and field of view. For current commercial technology and interfaces, a frame rate of 1kHz is only possible for fields of view of several 10's of square microns. However, high-speed "smart cameras" have recently been developed with integrated signal processing, where a programmable logic array measures the position of each particle[16] and only these positions, rather than the whole image, is passed to the data logging computer. Such systems can simultaneously measure the positions of several trapped particles[17] even when they are positioned far apart in the sample. Progress in both the commercial and research CMOS imagers is set to continue creating new opportunities for their use in optical tweezers.

Acknowledgments

This work was supported by the RCUK, AJW is supported by the Royal Academy of Engineering/EPSC.